

Optimization of Synchronous Buck-Boost DC-DC Switching Converter

Mahesh Gowda N M, S.S. Parthasarathy

Abstract—this paper presents a high-efficiency non-isolated synchronous buck-boost DC-DC switching converter. The circuit is made to operate in Discontinuous Conduction Mode (DCM) of operation for minimum inductor value, to reduce size and cost of the converter. A snubber capacitor is used across the switch to minimize turn-off loss. The power dissipation through snubber capacitor and inductor is minimized by proper selection of its value, hence improves the efficiency of the converter. Complementary gate signals are used to control the ON and OFF of main and auxiliary switch. By use of DCM of operation, complementary gate signals control scheme and snubber capacitor, turn-on loss is minimized. State space averaging method is used to obtain control-to-current transfer function. Using the transfer function module, Proportional Integral Derivative (PID) controller is tuned using PID tuner available in Simulink control design block to regulate load voltage and load current for change in inductor reference current (I^*), change in load and change in input voltage. The modules are verified using MATLAB Simulink simulator.

Keywords: DCM, buck, boost, non-isolated, PID controller, simulink.

I. INTRODUCTION

Switching DC-DC converters are considerable amount of the simplex power electronic circuits which transfer one level of electrical voltage into another level by switching action. These converters have obtained a greater considerable extent of concern in numerous fields like power supplies for individual computers, clerical device, telecommunication purpose, DC machine drives, aerodynamics, hybrid electric and fuel cell vehicles [1], renewable energy system etc. The analyses, regulate and stabilization of switching converters are the important circumstance that require to be taken into account. Many regulate types are utilized for control of switching DC-DC converters and the simple, straightforward and low amount regulate framework is forever in require for all industrial and large capability uses. Voltage-mode regulate and current-mode regulate are two commonly used regulate schemes to regulate the output voltage and current of dc-dc converters [2].

Feedback loop type automatically maintains a precise output voltage or current regardless of variation in reference voltage or current, load conditions, input voltage and current. Currently, there exist more than one different control approach, for example state space averaging type regulate [3], pulse width modulation and PID control technique [4], sliding

Mahesh Gowda N M, *Asst. Prof.*: Dept of Electronics and Communication Engg. PES College of Engineering Mandya, Karnataka, India

S.S. Parthasarathy, *Prof.*: Dept of Electrical and Electronics Engg. PES College of Engineering, Mandya, Karnataka, India

mode regulate [5], fuzzy logic regulate [6], etc. Each regulate type has its own benefits and disadvantages, and its efficient find out by the use where it is adopted.

In this proposed research work, we derived control-to-current transfer function module using state space averaging technique. Using derived transfer function module, PID values are obtained by tuning PID tuner available in Simulink Control Design Block to regulate load voltage and load current for change in inductor reference current, change in load and change in input voltage. The obtained P, I and D values are used in feedback PID controller of buck and boost modules. The buck and boost modules are tested for different conditions like change in inductor reference current, change in load and change in input voltage. For each case load voltage, load current, load power, inductor ripple current, efficiency and duty cycle are measured. From the obtained results it is noted that the theoretical and simulation measurement are comparable. The feedback controller works as expected.

II. PROPOSED SYSTEM

A non-isolated synchronous buck-boost DC-DC converter technology is to combine a buck mode and a boost mode converter. The converter is implemented to operate in discontinuous conducting mode (DCM) such that the inductor size, cost and converter size can be minimized. The DCM operation largely increases turn-off loss. This is one of the disadvantages of the inductor size reduction. The snubber capacitor added across the transistor switch is to reduce turn off loss. Snubber capacitor requires certain amount of energy stored in the inductor to discharge the capacitor energy before device is turned on. The major advantage of the DCM operation is minimum turn-on loss due to complementary gating signal control scheme and by use of snubber capacitor, thus low diode reverse recovery loss. Thus both soft switching turn-on and -off are obtained. The optimization of size, cost and efficiency can be done by selecting proper circuit parameters like snubber capacitor, inductor, switching device, and load resistor.

Fig. 1 is the proposed circuit topology. When $V_H = DC$ voltage source and $V_L = 0$ voltage, the circuit will act as buck mode with R_2 act as load and R_1 is the internal resistance of the V_H . When $V_H = 0$ and $V_L = DC$ voltage source, the circuit is in boost mode with R_1 as a load and R_2 is the internal resistance of V_L . In buck mode the inductor current is positive and in boost mode it is negative.

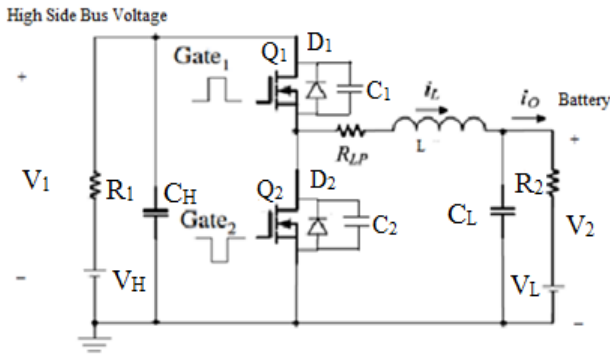


Fig.1: Synchronous Buck-BoostDC-DCSwitching converter.

III. POWER STAGE MODELING

The circuit shown in Fig.1 is used as buck and boost mode of operation. In this modes of operation there are two intervals, turn on and turn off as shown in Fig.2.

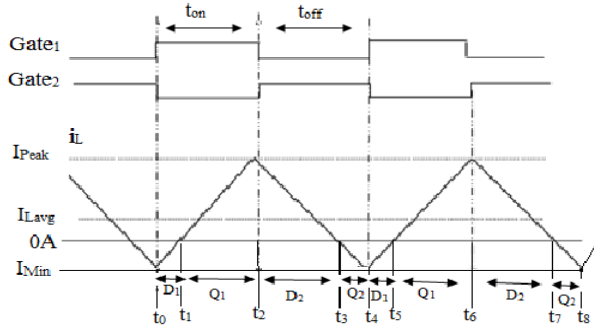


Fig.2: Inductor ripple current with turn-on and turn-off intervals

At time t_1 , Q_1 is on, the inductor current is positive, moving towards V_L and reach its peak value at time t_2 . At time t_2 , Q_2 is on and Q_1 is off, during this time, diode D_2 is carrying the freewheeling current. With the voltage V_2 against the inductor, the current reduces until it passes through zero and changes its direction. At this time (t_3) the current will flows through the auxiliary switch Q_2 . Now the diode D_2 turn off naturally without having reverse recovery loss. The parasitic ringing is also prevented. At time t_4 , Q_1 is on and Q_2 is off. During this time, diode D_1 will carry the inductor negative current. The voltage difference between V_1 and V_2 will appear across the inductor L , and the inductor current will increase towards positive direction and reaches zero at time t_5 and switch over to positive direction, and the main switch Q_1 takes the current. The cycle repeats.

Using state space averaging method, average inductor current (I_L), high side voltage (V_1), low side voltage (V_2) and control to current transfer function is derived and is given in equations (1-4).

$$I_L = \frac{DV_H - V_L}{R_1 D^2 + R_2 + R_p} \quad (1)$$

$$V_1 = \frac{V_H(R_2 + R_p) + DR_1 V_L}{R_1 D^2 + R_2 + R_p} \quad (2)$$

$$V_2 = \frac{D(V_H R_2 + DR_1 V_L) + R_p V_L}{R_1 D^2 + R_2 + R_p} \quad (3)$$

$$G_{id} = \frac{i_L}{d} = \frac{\left(s + \frac{1}{C_H R_1}\right) \left(s + \frac{1}{C_L R_2}\right) \frac{V_L}{L} - \frac{D I_L}{C_H L} \left(s + \frac{1}{C_L R_2}\right)}{\left(s + \frac{R_p}{L}\right) \left(s + \frac{1}{C_H R_1}\right) \left(s + \frac{1}{C_L R_2}\right) + \frac{D^2 \left(s + \frac{1}{C_L R_2}\right) s \left(1 + \frac{1}{C_H R_1}\right)}{L C_H}} \quad (4)$$

Where D = Duty cycle, V_H =voltage at high side, V_L =voltage at low side, R_1 =internal resistance of V_H in buck mode or load in boost mode, R_2 =internal resistance of V_L in boost mode or load in buck mode, $R_p = R_{dson} + R_{LP}$, R_{dson} =turn-on resistance of MOSFET, R_{LP} =parasitic resistance of inductor, C_H =input capacitor, C_L = output capacitor .

III. CURRENT FLOW DIRECTION

Current flow direction in buck and boost mode of operation is shown in Fig.3 (a) and (b) respectively. D_o is called zero current duty cycle, because at this value of duty cycle inductor current is zero and it is given by equation (5). Dis the control duty cycle.

$$D_o = \frac{V_L}{V_H} \quad (5)$$

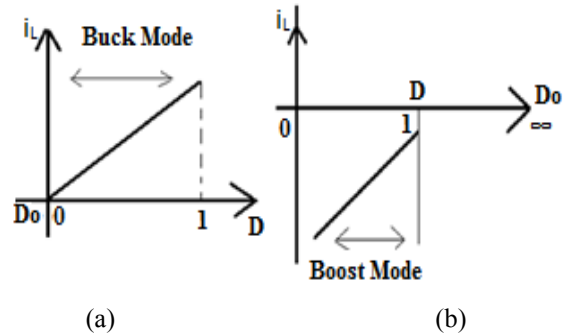


Fig.3: Current flow direction

In buck mode of operation $V_L = 0$, so $D_o = 0$, hence D is greater than D_o , which varies between 0 to 1 and the inductor current is positive. Here as D increases i_L also increases. In boost mode of operation $V_H = 0$, $D_o = \infty$, hence D is less than D_o which varies between 0 to 1 and the inductor current is negative. Here as D increases i_L approaches to zero.

V. EFFICIENCY MEASUREMENT

Power loss in DC-DC converter exist through the MOSFET conduction, diode conduction, MOSFET switching, inductor and through snubber capacitor. The efficiency of the converter is given in equation (6)

$$\eta = \left(\frac{P_o}{P_o + P_{sw-con} + P_{d-con} + P_{sw1} + P_{sw2} + P_L + P_{s-cap}} \right) \times 100 \quad (6)$$

Where P_o =output power, P_{sw-con} =switch conduction loss, P_{d-con} =diode conduction loss, P_{sw1} =loss during switch transition, P_{sw2} = loss during discharging of the drain to source capacitor of the MOSFET during turn on, P_L =inductor loss and P_{s-cap} =snubber capacitor loss.

VI. PID CONTROLLER

Proportional-Integral (PI) controller is used as a feedback controller with inductor current as a feedback reference as shown in Fig.4. Using transfer function of equation (4), P, I and D values are obtained by tuning PID tuner available in Simulink Control Design block as shown in Fig.5. Further P, I and D values are fine tuned by trial and error method for better transient response as shown in Fig.6. The corresponding transient response parameters are given in Table 1. Accordingly the P, I and D values are 0.000123, 60 and 0 respectively. Since D=0, PI controller is considered instead of PID controller.

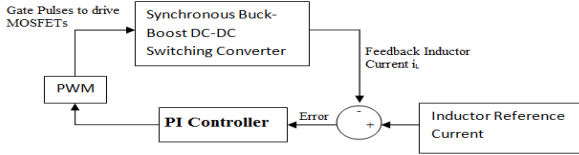


Fig.4: Feedback controller

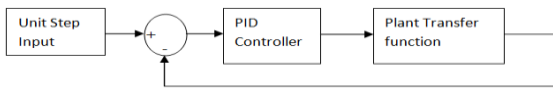


Fig.5: PID Tuner

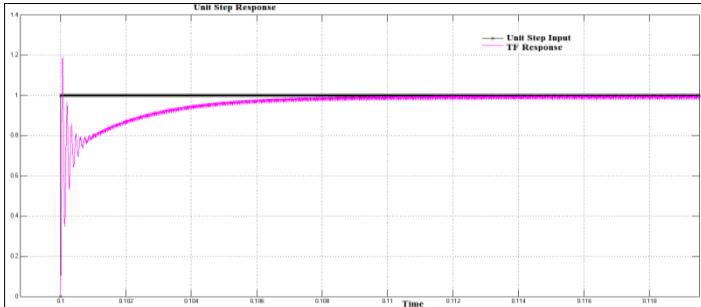


Fig.6: Transient response for step input.

Table 1: Transient response parameters for buck and boost mode

V_L (V)	V_H (V)	R_1 (Ω)	R_2 (Ω)	I^* (A)	t_r (sec)	t_s (sec)	% OS	e_{ss} (%)
0	250	10m	10	15	0.1m	8m	19	0.29
0	250	10m	10	20	0.1m	10m	18.5	0.29
0	250	10m	5	20	0.1m	5m	20.6	0.66
0	270	10m	10	15	0.1m	8m	21.7	0.29
60	0	18	10m	-12	0.1m	5m	29.7	0.14
60	0	18	10m	-16	0.1m	4m	40.4	0.16
60	0	9	10m	-12	0.1m	5m	-3.5	0.04
50	0	18	10m	-12	0.1m	5m	30.4	0.12

VII. RESULTS

I. Buck mode of operation:

Circuit parameters value is given in Table 2 (Ref Appendix-B)

Case 1: Change in inductor reference current:

Here the inductor reference current changes from 15A to 20A. A simulation result is shown in Fig.7 (Ref Appendix-A). With change in inductor reference current, the load current and load voltage increases and takes 4ms to reach steady state value. It is also noticed that as load current increases efficiency also increases as shown in Fig.8.

Case 2: Change in load resistance:

In this case load resistance changes from 10 Ω to 5 Ω and back to 10 Ω . A simulation result is shown in Fig.9 (Ref Appendix-A). The load current and load voltage also changes with change in load and takes around 3.5ms to reach steady state value. It is also noticed that as load resistance increases efficiency also increases as shown in Fig.10.

Case 3: Change in input voltage:

Here the input voltage changes from 250V to 270V. A simulation result is shown in Fig.11 (Ref Appendix-A). The load current and load voltage changes little bit with change in input voltage and takes 4ms to reach steady state value. It is also noticed that as input voltage increases efficiency decreases as shown in Fig.12.

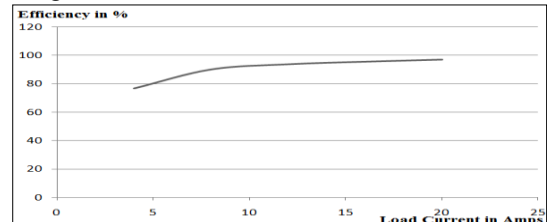


Fig.8: Efficiency v/s load current

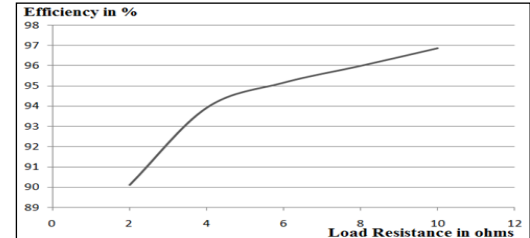


Fig.10: Efficiency v/s Load resistance

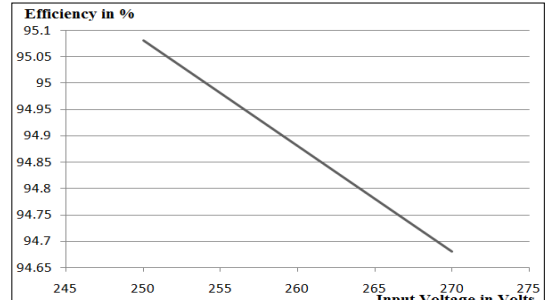


Fig.12: Efficiency v/s input voltage

The theoretical and simulation measurements of different parameters for above three cases are tabulated in table 3, 4 and 5 respectively (Ref Appendix-B) and they are comparable.

II. Boost mode of operation

Circuit parameters value is given in table 6 (Ref Appendix-B)

Case 1: Change in inductor reference current:

Here the inductor reference current changes from -12A to -16A. A simulation result is shown in Fig.13 (Ref Appendix-A). With change in inductor reference current, the load current and load voltage increases and takes 4ms to reach steady state value. It is also noticed that as load current increases efficiency decreases as shown in Fig.14.

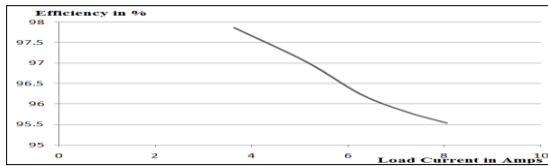


Fig.14: Efficiency v/s load current

Case 2: Change in load:

In this case load resistance changes from 18Ω to 9Ω and back to 18Ω. A simulation result is shown in Fig.15 (Ref Appendix-A). The load current and load voltage also changes with change in load and takes around 3ms to reach steady state value. It is noticed that as load resistance increases efficiency also increases and then decreases as shown in Fig.16.

Case 3: change in input voltage:

Here the input voltage changes from 50V to 60V. A simulation result is shown in Fig.17 (Ref Appendix-A). The

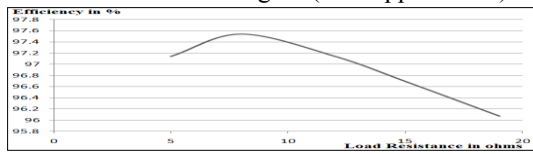


Fig.16: Efficiency v/s load resistance

load current and load voltage increases with change in input voltage and takes 4ms to reach steady state value. It is also noticed that as input voltage increases efficiency also increases as shown in Fig.18.

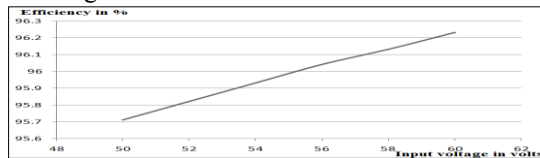


Fig.18: Efficiency v/s input voltage

The theoretical and simulation measurements of different parameters for above three cases are tabulated in table 7, 8 and 9 respectively (Ref Appendix-B) and they are comparable.

VIII. Conclusion

A high-efficiency non-isolated synchronous buck-boost DC-DC switching converter operating in DCM of operation and feedback controller technique is proposed in this paper. The Transfer Function module is derived and it is used to tune the PID controller using PID tuner available in Simulink Control Design block. The controller works as expected and the system feature can be predicted through simulation. In all the above six cases it is noticed the duty cycle changes smoothly without severe change, this smooth change of duty cycle leads to smooth current and voltage flow. The overall transition for load current and load voltage to reach steady state value takes around 3 to 4 ms for change in inductor reference current, change in load resistance and change in input voltage in both buck and boost converter. The simulation efficiency lies between 94.54 % to 96.92% in different test conditions.

References

- [1] Jih-Sheng Lai and D. J. Nelson, "Energy management power converters in hybrid electric and fuel cell vehicles," in Proceedings of IEEE, Industrial Electron, Taipei, Taiwan, Volume 95, Issue 4, April 2007, pp. 766 – 777.
- [2] S.Dhanasekaran, E.Sowdesh Kumar and R.Vijaybalaji, "Different Methods of Control Mode in Switch Mode Power Supply- A Comparison", International Journal of Advanced Research in Electrical, Electronics and Instrumentation Engineering, Vol. 3, Issue 1, January 2014
- [3] Mohammad Reza Modabbernia et al, "The State Space Average Model of Buck- Boost Switching Regulator Including all of The System Uncertainties", International Journal on Computer Science and Engineering (IJCSE) , Vol. 5 No. 02 Feb 2013
- [4] R.Sudha and Mr.P.M Dhanasekaran, "DC-DC Converters Using PID Controller and Pulse Width Modulation Technique", International Journal of Engineering Trends and Technology (IJETT) – Volume 7 Number 4- Jan 2014
- [5] H. Guldemir, "Modeling and Sliding Mode Control of Dc-Dc Buck-Boost Converter", 6th International Advanced Technologies Symposium (IATS'11), 16-18 May 2011, pp 475-480
- [6] K. Manickavasagam, "Fuzzy Logic Controller Based Single Buck Boost Converter for Solar PV Cell", International Journal of Applied Power Engineering (IJAPE), Vol. 3, No. 1, April 2014, pp. 1-8

Appendix-A: Figures

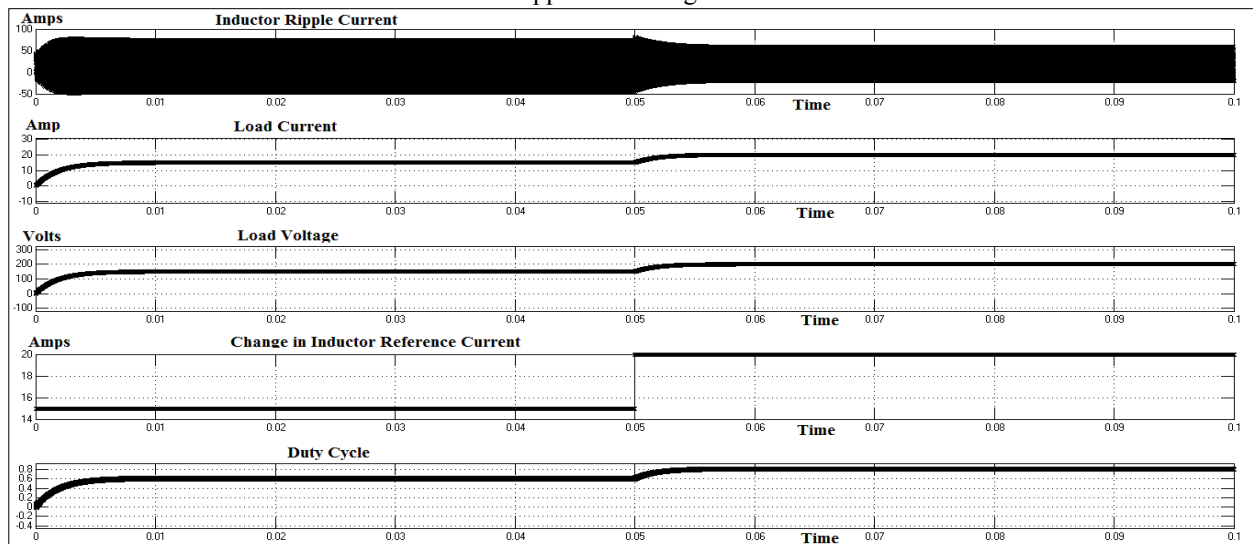


Fig.7: Buck Mode Inductor Ripple Current, Load Current, Load Voltage, Change in Inductor Reference Current and Duty Cycle.

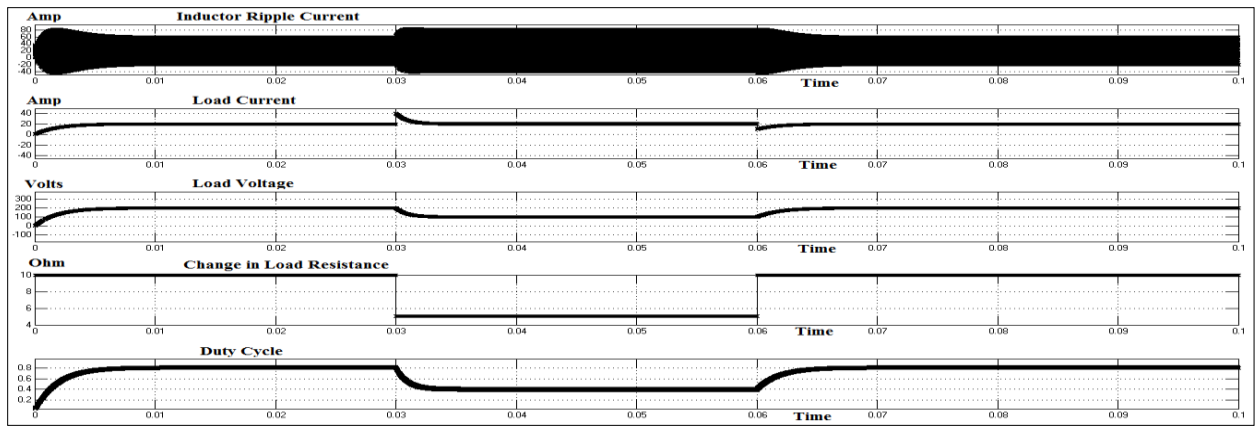


Fig.9: Buck Mode Inductor Ripple Current, Load Current, Load Voltage, Change in Load Resistance and Duty Cycle

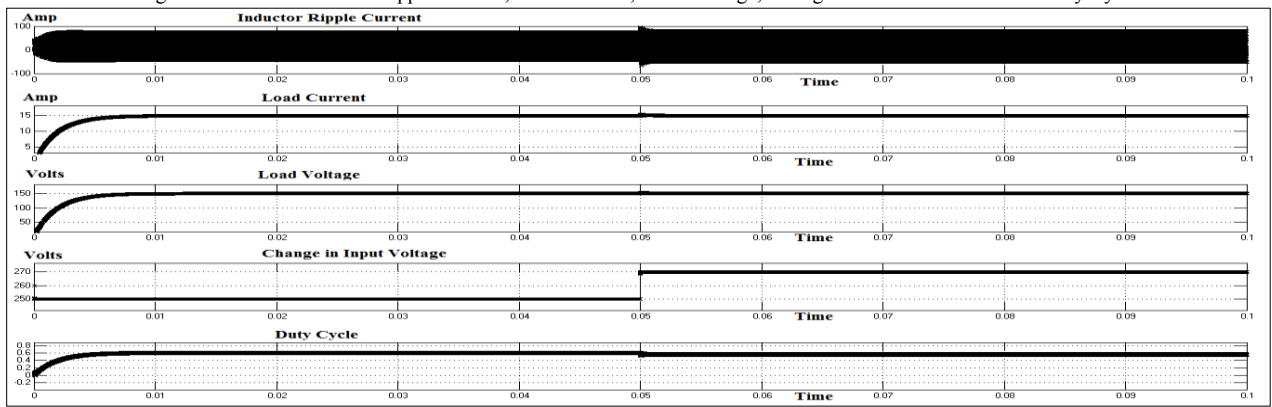


Fig.11: Buck Mode Inductor Ripple Current, Load Current, Load Voltage, Change in Input Voltage and Duty Cycle

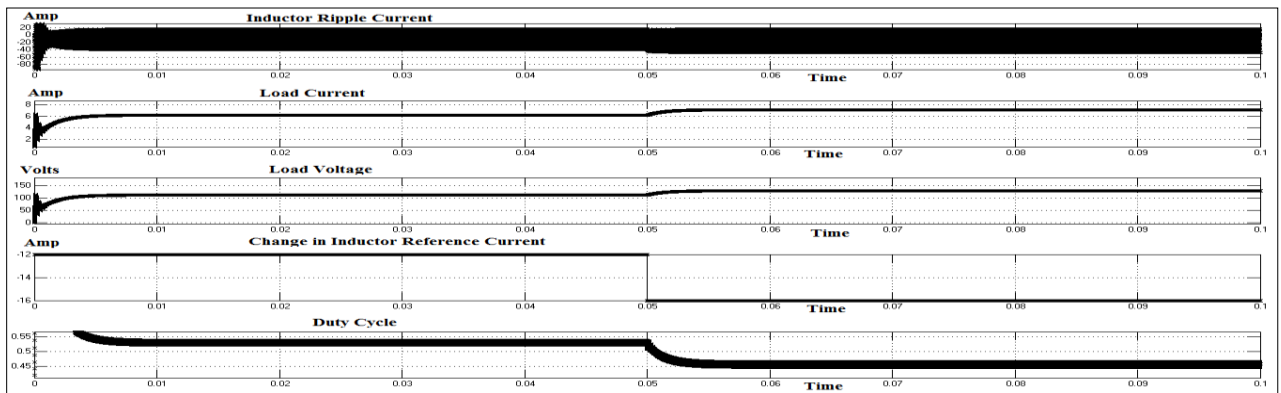


Fig.13: Boost Mode Inductor Ripple Current, Load Current, Load Voltage, Change in Inductor Reference Current and Duty Cycle

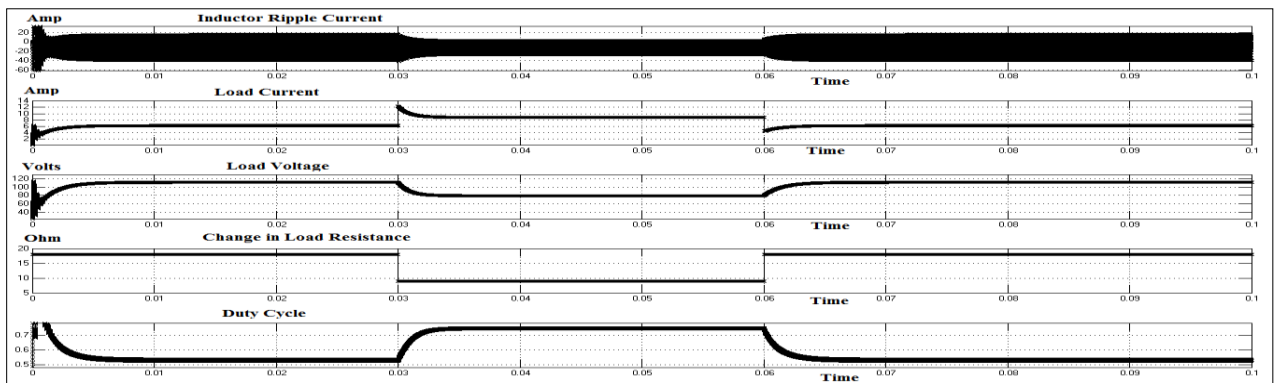


Fig.15: Boost Mode Inductor Ripple Current, Load Current, Load Voltage, Change in Load Resistance and Duty Cycle

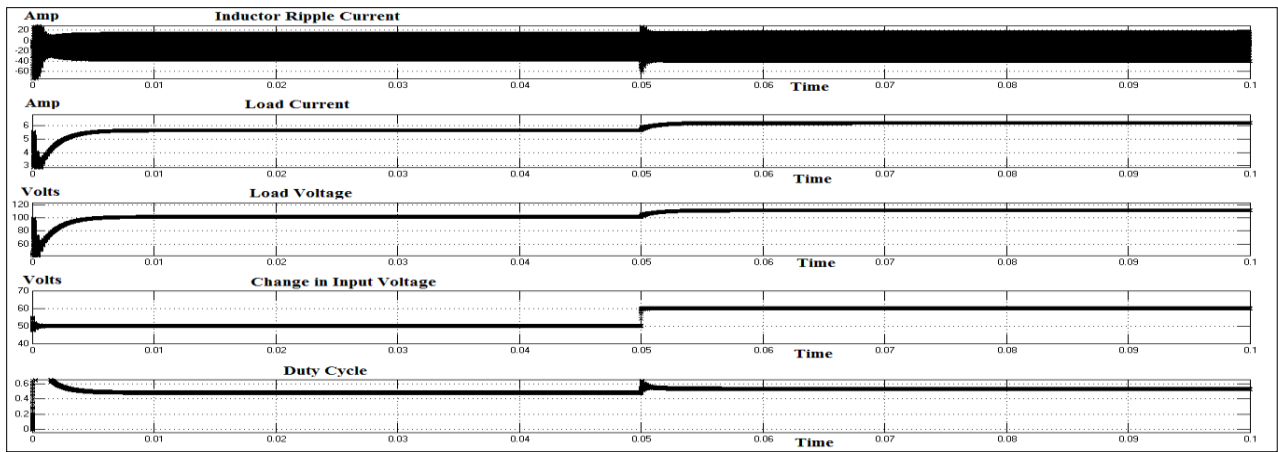


Fig.17: Boost Mode Inductor Ripple Current, Load Current, Load Voltage, Change in Input Voltage and Duty Cycle

Appendix-B: Tables

Table 2: Test parameter for buck mode

V_H	V_L	R_1	R_2	$C_H=C_L$	L	F_{sw}	R_{dson}	R_{LP}	Subber capacitor
250V	0V	10m Ω	10 Ω	150 μ F	10 μ H	50Khz	35m Ω	36m Ω	15nF

Table 3: Buck mode test parameters for change in inductor reference current

Parameters	$I^*=15A, R_L = 10\Omega, V_1 \approx 250V$		$I^*=20A, R_L = 10\Omega, V_1 \approx 250V$	
	Theoretical	Simulation	Theoretical	Simulation
V_2	150 V	150 \pm 1 V	200 V	200 \pm 0.8 V
I_2	15 A	15 \pm 0.1 A	20 A	20 \pm 0.1 A
$P_o = I_2 \cdot V_2$	2.25KW	2.25KW	4KW	4KW
Δi_L	60.21A	60A	40.91A	40A
η	95.08%	95.09%	96.86%	96.88%
D	60.45%	61%	80.62%	81.5%

Table 4: Buck mode test parameters for change in load

Parameters	$R_L = 10\Omega, I^*=20A, V_1 \approx 250V$		$R_L = 5\Omega, I^*=20A, V_1 \approx 250V$	
	Theoretical	Simulation	Theoretical	Simulation
V_2	200 V	200 \pm 0.77 V	100 V	100 \pm 1 V
I_2	20 A	20 \pm 0.078 A	20 A	20 \pm 0.2 A
$P_o = I_2 \cdot V_2$	4KW	4KW	2KW	2KW
Δi_L	40.91A	40A	59.70A	60A
η	96.86%	96.89%	94.64%	94.62%
D	80.62%	81%	40.58%	41%

Table 5: Buck mode test parameters for change in input voltage

Parameters	$V_1 \approx 250V, R_L = 10\Omega, I^*=15A$		$V_1 \approx 270V, R_L = 10\Omega, I^*=15A,$	
	Theoretical	Simulation	Theoretical	Simulation
V_2	150V	150 \pm 1 V	150 V	150 \pm 1 V
I_2	15 A	15 \pm 0.1 A	15 A	15 \pm 0.1 A
$P_o = I_2 \cdot V_2$	2.25KW	2.25KW	2.25KW	2.25KW
Δi_L	60.21A	60A	66.92A	66.66A
η	95.08%	95%	94.68%	94.70%
D	60.45%	60.5%	55.97%	56%

Table 6: Circuit parameters for boost mode.

V_H	V_L	R_1	R_2	$C_H=C_L$	L	F_{sw}	R_{dson}	R_{LP}	Subber capacitor
0V	60V	18 Ω	10m Ω	150 μ F	10 μ H	50KHz	35m Ω	36m Ω	15nF

Table 7: Boost mode test parameters for change in inductor reference current

Parameters	$I^*=12A, V_2 \approx 60V, R_L = 18\Omega,$		$I^*=16A, V_2 \approx 60V, R_L = 18\Omega,$	
	Theoretical	Simulation	Theoretical	Simulation
V_1	112.91V	110.3 \pm 0.3 V	130.02 V	127 \pm 0.4 V
I_1	6.27 A	6.13 \pm 0.03 A	7.22 A	7.06 \pm 0.02 A
$P_o = I_1 \cdot V_1$	707.94W	676.13W	938.74W	896.62W
Δi_L	28.12A	27.27A	32.30A	31.65A
η	96.23%	95.19%	95.80%	94.54%
D	52.28%	54%	45.15%	46%

Table 8: Boost mode test parameters for change in load

Parameters	$R_L = 18\Omega, I^* = -12A, V_2 \approx 60V,$		$R_L = 9\Omega, I^* = -12A, V_2 \approx 60V$	
	Theoretical	Simulation	Theoretical	Simulation
V_1	112.91V	110.3±0.3 V	79.84 V	79.2±0.3 V
I_1	6.27 A	6.13±0.02 A	8.87 A	8.8±0.03 A
$P_o = I_1 \cdot V_1$	707.94W	676.13W	708.18W	696.96W
Δi_L	28.18A	27.36A	14.97A	14.54A
η	96.23%	95.19%	97.49%	96.92%
D	52.28%	54%	73.93%	75%

Table 9: Boost mode test parameters for change in input voltage

Parameters	$V_2 \approx 50V, R_L = 18\Omega, I^* = -12A$		$V_2 \approx 60V, R_L = 18\Omega, I^* = -12A$	
	Theoretical	Simulation	Theoretical	Simulation
V_1	102.9V	100.5±0.3 V	112.91 V	110.3±0.3 V
I_1	5.71 A	5.58±0.02 A	6.27 A	6.13±0.02 A
$P_o = I_1 \cdot V_1$	587.55W	560.79W	707.94W	676.13W
Δi_L	25.70A	25.12A	28.12A	27.36A
η	95.71%	94.30%	96.23%	95.16%
D	47.64%	49%	52.28%	53.5%